EUMETSAT/ECMWF Fellowship Programme
Research Report No. 33

Impact assessment of GOES-15 CSR and Meteosat-10 ASR in the ECMWF system

Cristina Lupu and Anthony P. McNally

January 2014

Series: EUMETSAT/ECMWF Fellowship Programme Research Reports

A full list of ECMWF Publications can be found on our web site under:
http://www.ecmwf.int/publications/

Contact: library@ecmwf.int

1 Executive summary

The constellation of operational geostationary satellites include satellites at 0°longitude and 57°E (operated by EUMETSAT), a satellite at 140°E (operated by JMA), and satellites at 135°W and 75°W (operated by NOAA). This report describes activities related to the maintainance and evolution of the geostationary network of clear and cloudy radiances assimilated in the ECMWF operational suite and the main results from research work carried out to study the growth rate of the model humidity errors within the 4D-Var window. The main operational changes in the geostationary network are listed below:

- **Operational assimilation of clear-sky radiances (CSR) from GOES-15 since 24 April 2012:** GOES-15 CSR have been successfully introduced in the operational cycle 37R3 on 19 January 2012 and monitored in ECMWF operations until late April 2012. Three months of monitoring experiments have shown that GOES-15 CSR are stable data, with a small bias which can be globally corrected. Assimilation experiments with WV CSR from GOES-15 slightly improve the model fit to radiosonde relative humidity over the Southern Hemisphere and Tropics. The impact of using GOES-15 WV CSR on medium-range forecasts is overall neutral to slightly positive.

- **Operational assimilation of all-sky radiances (ASR) from Meteosat-9 since 19 June 2012:** The all-sky assimilation of SEVIRI radiances has been succesfully introduced within the ECMWF operational system model cycle 38R1 to assimilate Meteosat-9 radiances in overcast conditions, in addition to the data in clear sky conditions.

- **Operational assimilation of ASR from Meteosat-10 since 5 February 2013:** Meteosat-10 ASR have been disseminated in parallel with the operational Meteosat-9 ASR since the end of October 2012, and monitoring the data quality started immediately at ECMWF taking advantage of all the developments implemented into the IFS for the assimilation of Meteosat-9 ASR. The biases in the ASR from Meteosat-10 are lower than that from Meteosat-9 and in other respects the quality is the same.

At the time of writing, ASR from Meteosat-10 and CSR from Meteosat-7, GOES-13/15 and MTSAT-2 are operationally assimilated at ECMWF. Depending on the instrument, one or two channels peaking in the water vapour absorption band are used, with maximum sensitivity in the mid-to-upper troposphere.

Observations sensitive to temperature and moisture can produce wind increments through the dynamic response to temperature and moisture increments in 4D-Var. Although in recent years work has been mainly carried out to understand the wind tracing capability of humidity-sensitive geostationary radiances in the 4D-Var (Lupu and McNally, 2012), in the last year, one of the research highlights was the application of the 4D-Var methodology to time varying ozone-sensitive radiances.

SEVIRI ozone-sensitive radiances have been evaluated within the ECMWF operational system, both in terms of possibility of wind extraction from the 4D-Var assimilation and in terms of impact on analysis and forecast. The findings of this investigation are detailed in Lupu and McNally (2013) and show that, if the dynamical link between the ozone and the rest of the system is enabled, the 4D-Var has the freedom to change the temperature and wind fields, as well as the ozone field itself in order to improve the fit to observed ozone concentrations. Experimentation with SEVIRI ozone-sensitive radiances in the context of a full observing system improves the fit to other infrared ozone-sensitive radiances. Wind analysis and forecast impacts results do not suggest benefit on improving the operational ECMWF wind field, and as a result SEVIRI ozone-sensitive radiances are not currently assimilated at ECMWF.

Continuous efforts are made to fully understand the behaviour of infrared instruments in the assimilation in order to improve their impact on model analyses and forecasts. Work to investigate the feasibility of exploiting the geostationary radiance data to study the growth rate of the model humidity errors within the 4D-Var window has also started.

This report presents a summary of recent events occured in the geostationary network (Section 2) and describes the testing and implementation in ECMWF operations of GOES-15 CSR (Section 3) and Meteosat-10 ASR (Section 4). Results from an investigation of the model error growth rate in 4D-Var window with humidity sensitive SEVIRI CSR are discussed in Section 5. Finally, our conclusions and future plans on exploiting the geostationary radiances are summarized in Section 6.

2 Recent events and operational changes in the use of geostationary radiances

The most important events occured in the geostationary satellite network during 2012-2013 are listed below.

a) NOAA's GOES satellites

- **GOES-11-15 transition:** To keep operations running smoothly, GOES-11 operational since 2006 as GOES-West satellite, has been replaced by GOES-15, NOAA's newest geostationary satellite.
- **GOES-13 outage:** One of the most noteworthy events last year was the outage of GOES-13 satellite following increasead amounts of noise observed in imagery on 23th September 2012. The satellite was put in stand-by mode until 18th October 2012, when tests of GOES-13 instrumentation have demonstrated the imager is ready to return to GOES-East operational service. The main cause of the GOES-13 anomaly was a motor vibration in the sounder filter wheel subsystem that was transmitted on to the imager and sounder optical bench (*NOAA communicate*). The return of GOES-13 to operational service optimizes the long term continuity of the GOES constellation.
- **GOES-14 temporary replaced malfunctioning GOES-13:** During the GOES-13 outage, NOAA has placed its backup GOES-14 satellite located over 105°W into service. An eastward drift maneuver of 0.90°per day was initiated on 1st October 2012 and conducted until 19th October 2012, when GOES-14 arrived at 89.5°W. After GOES-13 returned to the operational service, a drit maneuver to the West of 0.34°per day has been conducted between 19th December 2012 and 6th February 2013 to relocate GOES-14 at 105°W, where it will remain in stand-by mode until recalled because of anomalies of any of GOES operational satellites.

At ECMWF, the IFS forecast model has been modified to ingest the GOES-14 CSR and AMVs data sets. Based on operational passive monitoring statistics of GOES-14 CSR from 2nd October 2012 to 17 October 2012 we concluded that the general quality of clear-sky radiances from GOES-14 satellite is similar to the quality of the GOES-13 radiances (not shown). The ECMWF 4D-Var analysis system is prepared to monitor and assimilate GOES-14 radiances and AMVs if required. Assimilation experiments performed to operationally assimilate GOES-15 radiances are detailed in Section 3.

b) EUMETSAT geostationary satellites

- **Swap of prime satellites for 0°:** Meteosat-10 replaced Meteosat-9 as prime operational geostationary satellite, following a relocation from 3.4°W to 0°. Meteosat-9 has been relocated from 0°to 9.5°E and made the prime satellite for the Rapid-Scanning Service. Meteosat-8 is the backup satellite to Meteosat-10 and Meteosat-9, to be used in case of a problem occuring with either of these satellites.

In 2012-2013, the availability of clear and all-sky radiances from Meteosat-7 and Meteosat-9 satellites has been excellent. Meteosat-7 CSR were continuously assimilated in ECMWF operations, while the availability of Meteosat-9 was impacted by orbital manoeuvres - the East-West Station Keeping Manoeuvre (February 21-26, 2012) and the North-South Manoeuvre (25 June-3 July 2012).

Following the succesful launch of the Meteosat-10 satellite, ASR from the calibration-validation phase has been arriving routinely at ECMWF since the end of October 2012. An evaluation of Meteosat-10 ASR in the ECMWF system is provided in Section 4.

c) JMA geostationary satellites

- **Maintenance of the MTSAT's ground system:** JMA conduct an annual maintenance of the MTSAT's ground system every year between October and December. This is needed because of a problem in the MTSAT-2 satellite's ability to relay the Low Rate Information Transmission (LRIT) information to remote users.

During the system maintenance, MTSAT-1R was brought back into operation and ECMWF restarted receiving MTSAT-1R CSR and AMVs from 18th October to 26th December 2012. Operational monitoring of MTSAT-1R CSR has began as soon as data became available aiming at re-assessing the quality of the data and to spun-up the VarBC predictor parameters. The monitoring was resumed from 30th October 2012 and CSR from MTSAT-1R re-assimilated in ECMWF operations until the end of the operational service by MTSAT-1R. A similar procedure has been applied to re-assimilate MTSAT-2 CSR data in operations, at the end of the maintenance period (monitoring from 15th January 2013, followed by assimilation since 5th February 2013). Additionally MTSAT-1R and MTSAT-2 CSR and AMVs BUFR format were changed from FM-94 BUFR edition 3 to edition 4 on 31st October 2012.

3 Impact of GOES-15 CSR on ECMWF analyses and forecasts

3.1 Introduction

On 6th December 2011, GOES-15 replaced GOES-11 and has been declared GOES-West satellite in the NOAA Geostationary Operational Environmental Satellite constellation. NOAA's operating strategy calls for two GOES satellites to be active at all times, one satellite to observe the Atlantic Ocean and the eastern half of the U.S.A., and the other to observe the Pacific Ocean and the western part of the country. GOES-13 (or GOES-East) positioned at 75°W longitude and GOES-15 (or GOES-West) positioned at 135°W longitude are currently, the two operational meteorological satellites in geostationary orbit over the equator operates by NOAA. Additionally, GOES-12 supports Central and South America to prevent data outages during the GOES-13 rapid scan operations and GOES-14 is maintaining as on-orbit spare to replace either, GOES-15 or GOES-13, in the event of failure.

Launched in 2010, GOES-15 is the final spacecraft in the latest GOES-N/O/P series of NOAA geostationary satellites. Changes to the GOES five band imager from GOES-11 through GOES-15 include some differences in spectral band and differences in the nominal spatial resolution between the two versions of the GOES Imager as following:

- The 6.7 μm water vapor channel on GOES-11 imager was replaced by a much broader 6.5 μm water vapor channel on GOES-15.
- The spatial resolution was increased to 4 km for all IR bands.
- 12 μm IR channel was replaced by the 13.3 μm IR channel.
- The improved battery enables normal operation throughout the semiannual eclipse that occur around the solstices.
- The GOES-15 imager visible channel is a narrower channel that is centered at 0.63 μm compared to the broader 0.65 μm visible channel on GOES-11.

Clear-sky radiances from GOES-15 have been produced by the Cooperative Institute for Meteorological Satellite studies (CIMSS, Madison, USA) and have been received at ECMWF in near real time since December 2011. Technical modifications have been made to the IFS model cycle 37R3 to support the monitoring and assimilation of GOES-15 radiances.

3.2 Monitoring statistics

The GOES-15 CSR were evaluated in the ECMWF operations through a monitoring experiment which covered 3 months (January to April 2012). Figure 1 shows the time series of first guess and analysis departures statistics before and after bias correction for all GOES-15 CSR in the WV channel. Biases which may result from forecast model error, radiative transfer model error, or measurement error are removed using a variational bias correction scheme (VarBC, Dee, 2004). Bias predictors used for clear-sky radiances from geostationary satellites are a flat global offset, 1000-300 hPa and 200-50 hPa layer thicknesses and total precipitable water. The analysis of first guess departures of passive monitored GOES-15 CSR has shown the data to be of generally of good quality. The systematic biases were found to be stable and they were corrected by VarBC.

The GOES-15 satellite encountered two important anomalies in March 2012:

- Imager calibration issue for WV band during March 12-16, 2012: Passive monitoring of GOES-15 CSR in ECMWF operations indicated a sudden change in the bias in the WV band from 12 to 16 March 2012. We reported the issue to Dr Tim Schmit (NOAA/NESDIS) and a correction has been applied to the calibration parameters for GOES-15 imager. More details on the GOES-15 imager calibration issue are available at: http://cimss.ssec.wisc.edu/goes/blog/archives/9995.
- GOES-15 satellite went into a sun acquisition mode and stopped transmitting data during March 21-23, 2012.

For the period after the data outage, the radiances for WV channel appear to be stable, with no significant trends over the period.

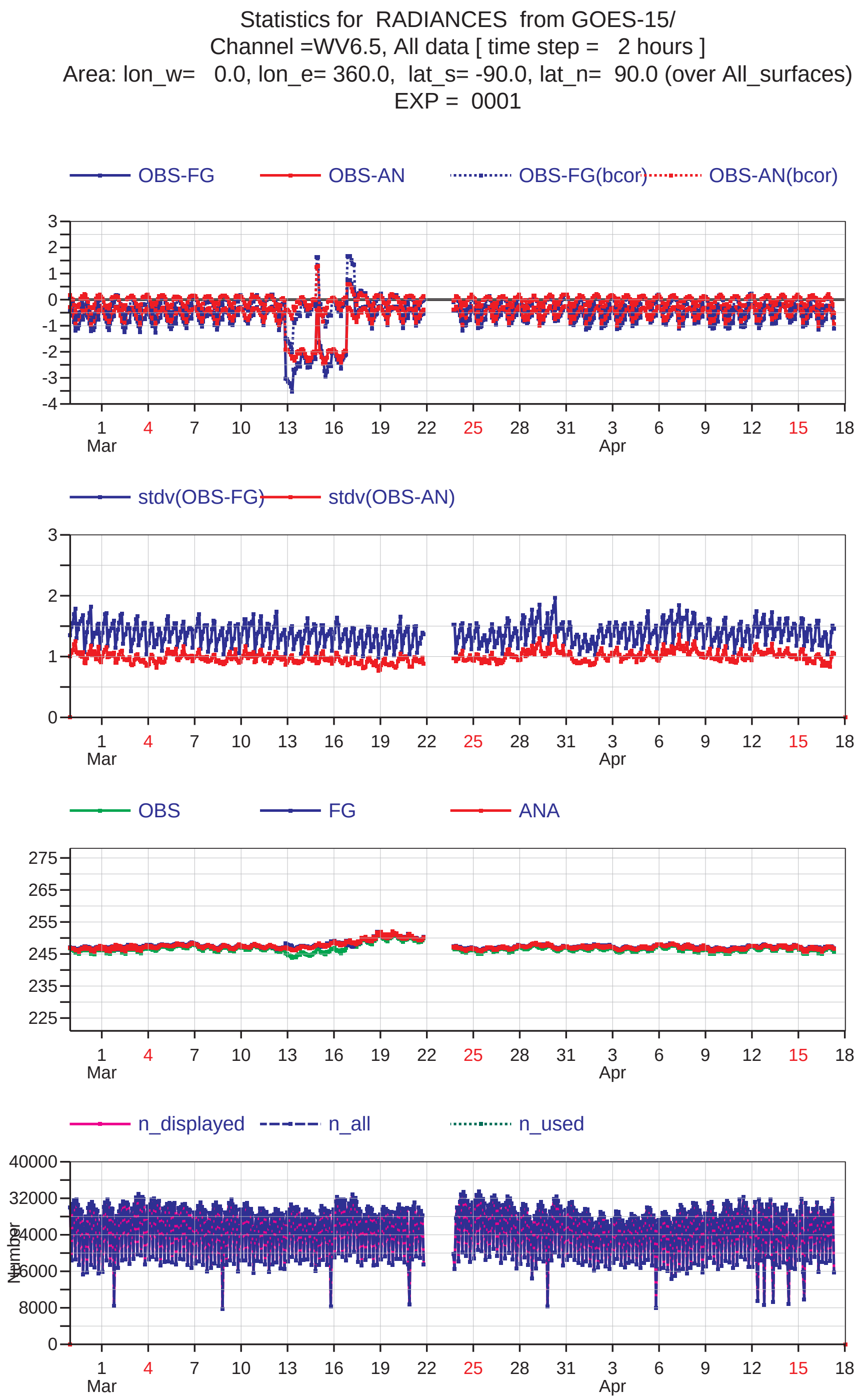

Figure 1: Time series of first-guess and analysis departure statistics, in K, for the passive monitoring of GOES-15 WV CSR in ECMWF operations from 1 March to 18 April 2012.

3.3 Impact assessment

The assimilation strategy of CSR from GOES-15 follows the one used for the assimilation of GOES-13 CSR and has been discussed in detail by Lupu and McNally, (2011). Three assimilation experiments with GOES-15 CSR were run at T511 horizontal resolution and 91 vertical levels in a 4D-Var 12-hour assimilation window in order to evaluate the impact of CSR from GOES-15 on the analysis and forecast:

- **Control**: use all conventional and satellite observations operationally assimilated in cycle 37R3 except for GOES-15 CSR that are passivelly monitored;
- **GOES-15 restricted**: clear-sky water vapour radiances from GOES-15 were assimilated in addition to the set of observations used in the **Control** experiment. This experiment follows the current blacklist criteria applied to GOES-13 CSR, and consequently exclude GOES-15 CSR during several hours in the night (*i.e.*, 1:30 UTC to 8:30 UTC).
- **GOES-15**: differs from the previous experiment **GOES-15 restricted** by the fact that GOES-15 CSR are also assimilated during the night.
- **GOES-13 revised**: differs from the experiment **GOES-15** by the fact that also GOES-13 CSR are also assimilated during the night.

3.3.1 Analysis impact

Figure 2 shows the evolution of the background and analysis departures as well as the bias corrected differences for the assimilated GOES-15 CSR in the WV channel from **GOES-15** experiment over two month period. When GOES-15 WV radiances are assimilated, the background fit has a mean standard deviation of about 1.22 K, while the mean standard deviation of analysis fit is 0.7 K. There are 29.5% more GOES-15 CSR assimilated in **GOES-15** experiment than in **GOES-15 restricted** experiment. The changes to bias correction and mean departures are consequently slightly different between those experiments (not shown). The analysis of **GOES-15** and **GOES-15 restricted** experiments compared with the Control neither showed negative impact on the fit to other observations and bias corrections. Figure 3 shows that the assimilation of GOES-15 CSR slightly improve the model fit to radiosonde relative humidity over the Southern Hemisphere and Tropics.

3.3.2 Forecast impact

Forecast verification has been done against each experiment's own analysis. Figure 4 shows the normalized difference in geopotential RMS error for the Southern Hemisphere, Tropics and Northern Hemisphere at 200 hPa, 500 hPa, 850 hPa and 1000 hPa. Comparing **GOES-15** experiment to **Control** (black line) isolates the impact of assimilating GOES-15 CSR, while comparing **GOES-15 restricted** experiment to **Control** (red line) illustrates the impact of the reduced GOES-15 CSR dataset. In general, the use of GOES-15 CSR has a positive impact by reducing the RMS errors on 500 hPa geopotential. The largest positive impact is seen for the **GOES-15** experiment. Similar impacts can be seen on mean tropospheric forecast scores for wind, relative humidity and temperature (not shown).

Figure 5 shows zonal plots of the normalised difference **GOES-15** minus **Control** of the RMS wind error at forecast lengths ranging from 12-hour to 192-hour. There is significant decrease in vector wind RMS error at 60°N at levels between 300 hPa and 700 hPa, reaching locally 1% at 72-hour forecast. As there

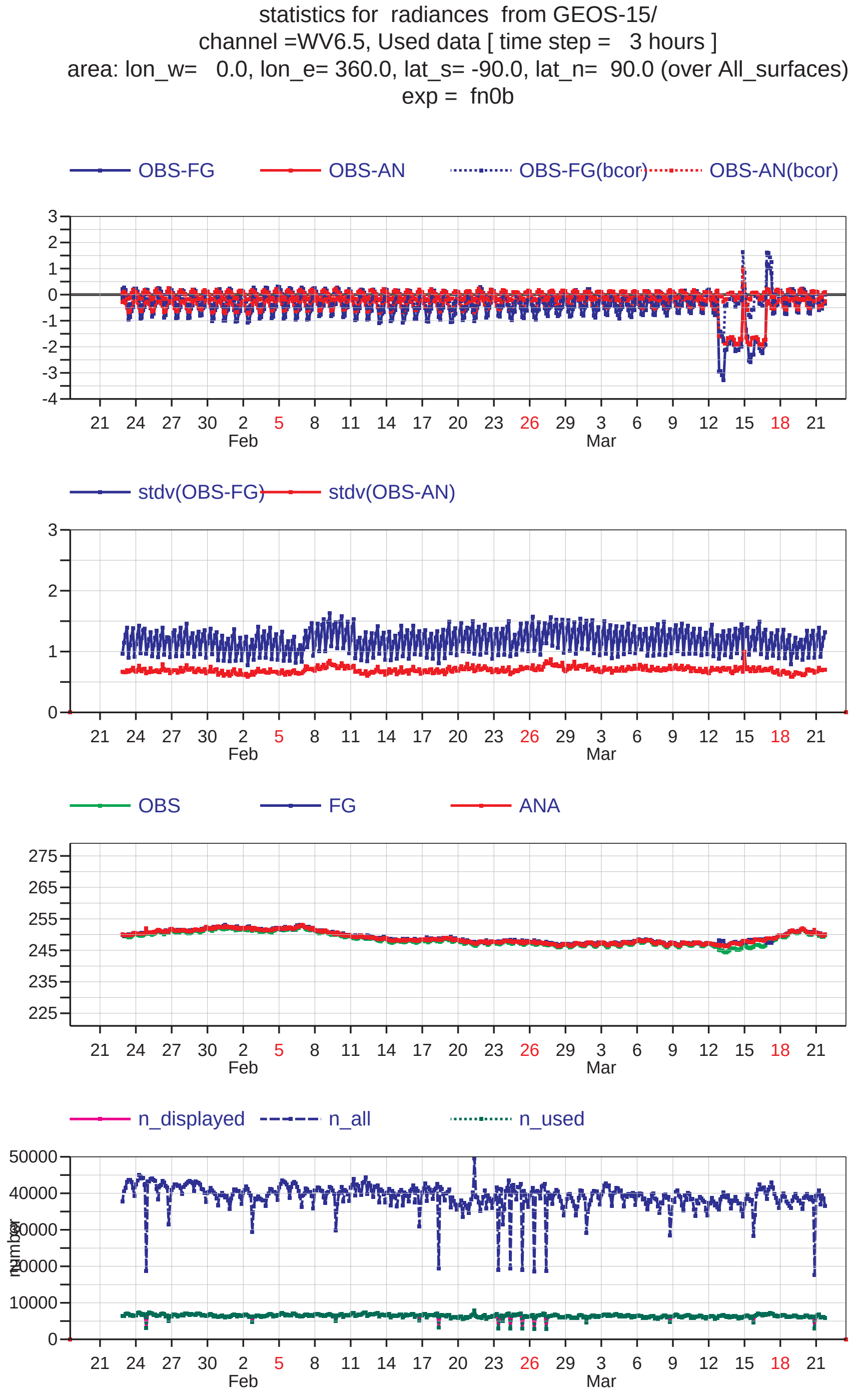

Figure 2: Time series of first-guess and analysis departure statistics, in K, for the active assimilation of GOES-15 WV CSR from 23 January to 23 March 2012.

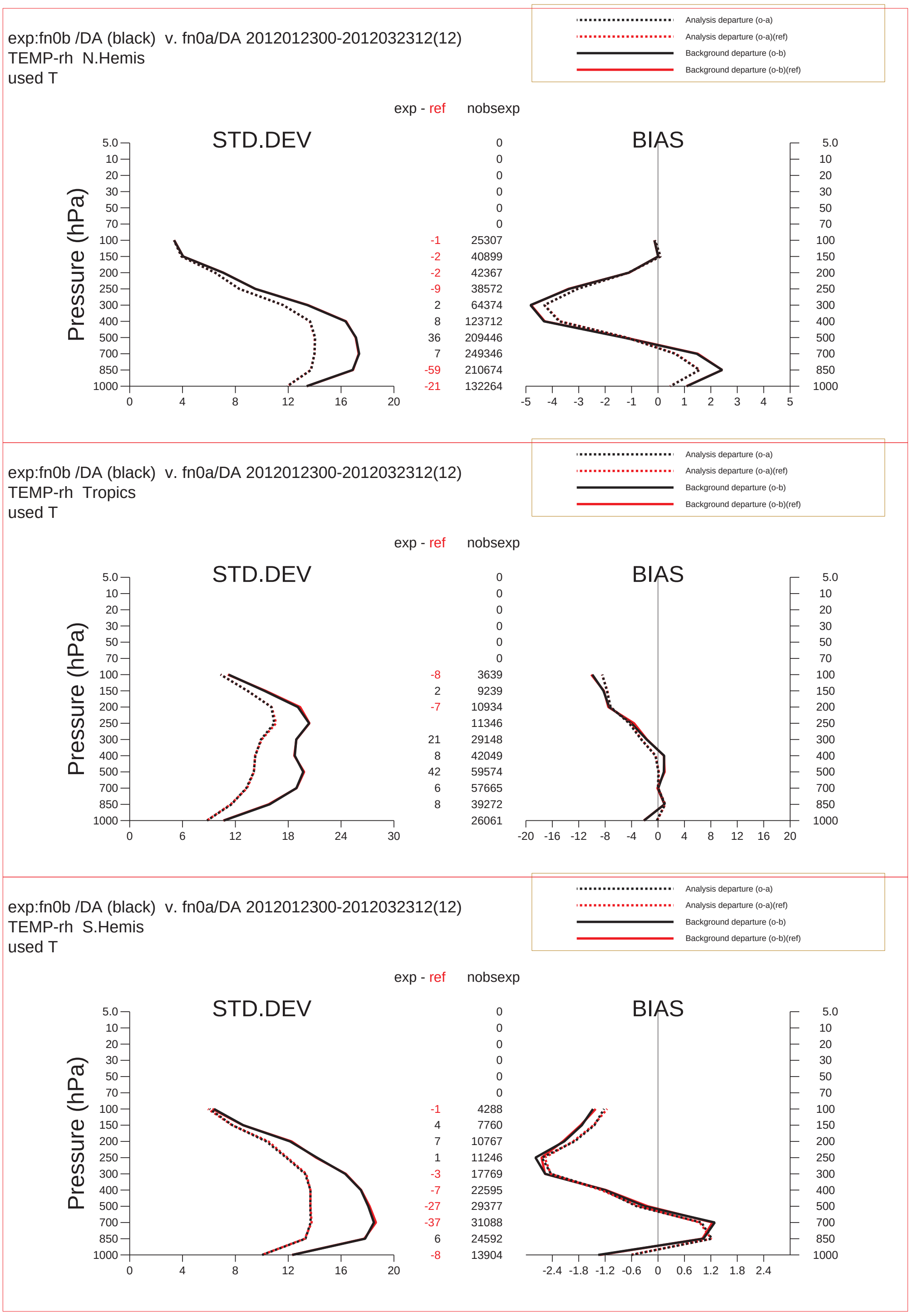

Figure 3: Standard deviation (left) and bias (right) for the departures of used radiosonde relative humidity in the Northern Hemisphere extratropics (top), Tropics (middle) and in the Southern Hemisphere extratropics (bottom) from the background (solid) and analysis (dotted) for the GOES-15 CSR assimilation (black) and the Control (red). "nobsexp" correspond to the number of observation assimilated in GOES-15 experiment and the numbers in exp-ref correspond to the difference in number of observations between GOES-15 and Control experiments.

are no significant differences in geopotential forecast scores from GOES-15 and GOES-15 restricted experiments, we will not restrict the GOES-15 CSR data usage as previously done for GOES-13 CSR.

With the new operational GOES-West satellite, we took the opportunity to re-assess the impact of GOES-13 CSR in forecast scores. In the actual operational configuration, water-vapour CSR from GOES-13 are blacklisted between 1:30 UTC and 8:30 UTC). The experiment **GOES-13 revised** aims to evaluate if this restriction could be removed now, with the new operational configuration of geostationary system. From 5, it appears that the RMS error in geopotential slightly increase when comparing the GOES-13 revised (green line) and the GOES-15 (black line) experiments. Since the results of the reviewed GOES-13 data selection does not appear to improve more the forecast scores, we do not suggest an operational change to the current configuration of GOES-13 CSR.

4 Meteosat-10 ASR: Initial assessment

On 5th July 2012, EUMETSAT launched MSG-3 the third in a series of four satellites introduced in 2002. The satellite's main payload is the optical imaging radiometer SEVIRI, that observes the Earth's atmosphere and surface through twelve spectral channels and provide measurements with 15 minutes temporal resolution and 3 km spatial resolution at the subsatellite point (Schmetz *et al.*, 2002). The MSG-3 satellite completed its in-orbit testing on 12 December 2012 and it was renamed Meteosat-10.

At ECMWF we have started to use operationally the ASR from Meteosat-9 since 19 June 2012 and stopped using the CSR. Taking advantage of all the developments made for Meteosat-9 ASR, preparations have been done for monitoring and assimilation of Meteosat-10 ASR in the IFS cycle 38R1. Parallel dissemination of ASR products with those from Meteosat-9 allowed cross-checking of data quality between the two satellites.

An off-line experiment in which ASR from Meteosat-10 were passively monitored has been initially run using ECMWFs 12-h 4D-Var system, with a spatial model resolution of T319 (60 km), an incremental analysis resolution of T255 (80 km) and 91 levels in the vertical and the full observing system assimilated operationally over the period 1st to 30 November 2012. Figure 6 shows comparison between time series of mean and standard deviations of the first-guess and analysis departures for all-sky SEVIRI radiances from Meteosat-9 and MSG-3 in WV channel at 6.2 μm. Side by side comparison of the two sets of data showed that mean first-guess and analysis departure statistics are reduced for MSG-3 data. Comparisons between standard deviations of first-guess and analysis departures indicate that in the water vapour channel the two sets of data have a similar level of noise. The MSG-3 SEVIRI instrument appeared to be performing well and the first evaluation of data has demonstrated that the radiances have reduced biases relative to data from Meteosat-9.

Parallel monitoring of Meteosat-10 and Meteosat-9 ASR on ECMWF operations has been performed from 30th October 2012 to 15 January 2013 and from 23 January 2013 to 5 February 2013, allowing the spin-up of the variational bias correction (VarBC) coefficients, and the monitoring of data. As the zenith angle and subsatellite point information are not included yet in the ASR BUFR file, we had to temporarily stop the operational monitoring during the Meteosat-10 satellite relocation from 3.4°W position to the 0°position.

The active use of Meteosat-9 ASR in ECMWF operations has been resumed on 17th January 2013, when the satellite start drifting toward 9.5°E. We operationally assimilate Meteosat-10 ASR in ECMWF 4D-Var system since 5th February 2013. Routine monitoring and assessement of ASR from Meteosat-10 show that geostationary ASR remain healthy in operations (Fig. 7) .

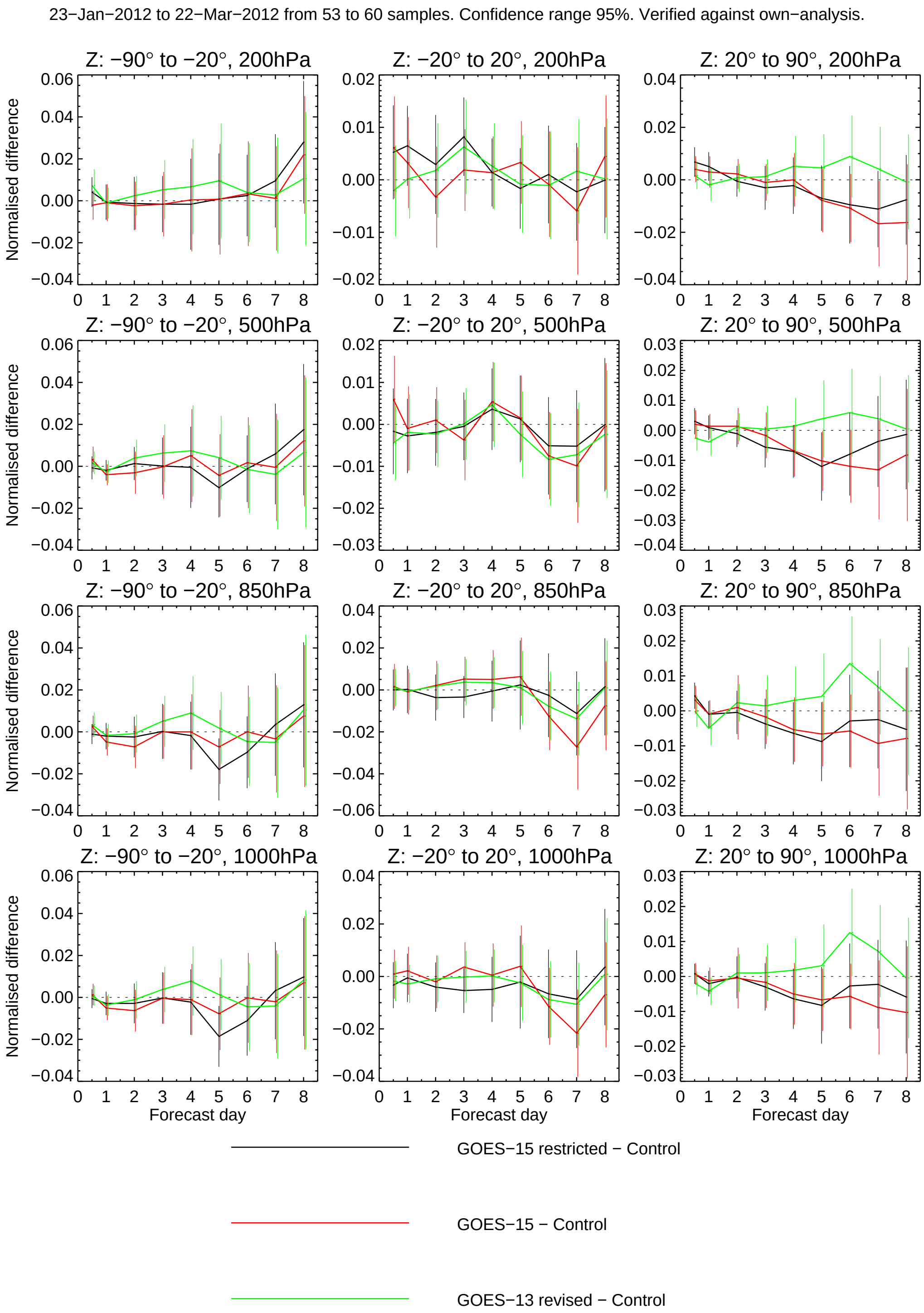

Figure 4: Normalised differences in the root mean square forecast error for the 200 hPa, 500 hPa, 850 hPa and 1000 hPa geopotential over the Southern Hemisphere extra-Tropics (first column), Tropics (second column) and Northern Hemisphere extra-Tropics (third column) between GOES-15 restricted and Control (red line), GOES-15 and Control (black line) and GOES-13 revised and Control (green line) as a function of forecast range in days. All experiments have been verified against own analysis. Negative values indicate a reduction in forecast error for the experiment. Error bars indicate confidence intervals at the 95% confidence level.

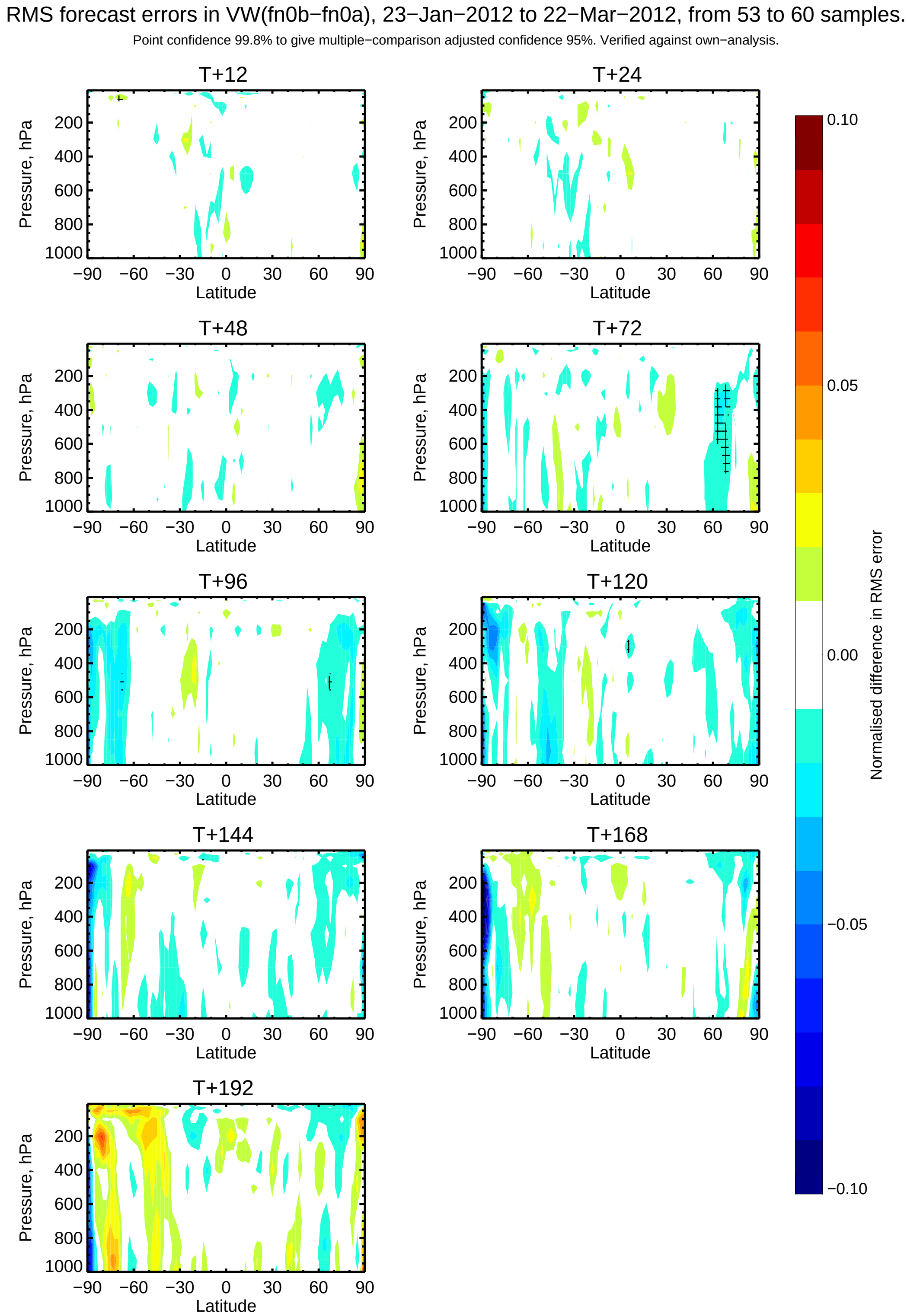

Figure 5: Zonal means of normalised differences in the root mean square forecast error for vector wind between GOES-15 experiment and the Control. Blue shading indicates an improvement in the GOES-15 experiment compared to the Control. Forecasts are verified against own analyses from the respective experiment. Scores are shown for the period 23 January to 23 March 2012. Each panel shows the differences for the forecast range indicated above the panel.

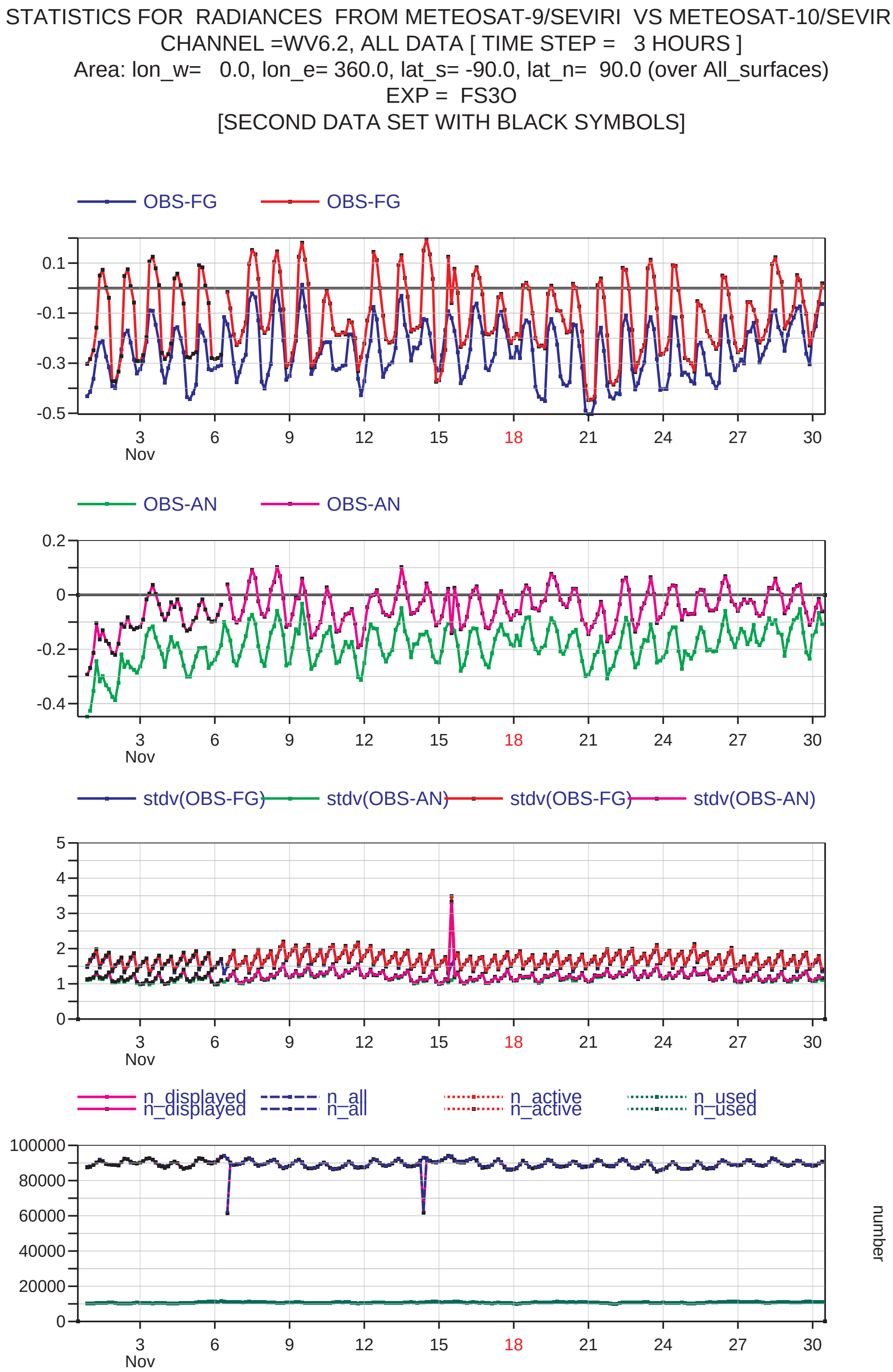

Figure 6: Statistics for radiances from Meteosat-9 and MSG-3 for the WV channel at 6.2 µm over the period 1 November-30 November 2012. Panel 1: Time series of mean first-guess departures (before bias correction) for ASR from Meteosat-9 (blue) and MSG-3 (red). Panel 2: Time series of mean analysis departures (before bias correction) for ASR from Meteosat-9 (green) and MSG-3 (magenta). Panel 3: Standard deviations of the first guess and analysis departures for ASR from Meteosat-9 and MSG-3. Panel 4: Time series of observation numbers.

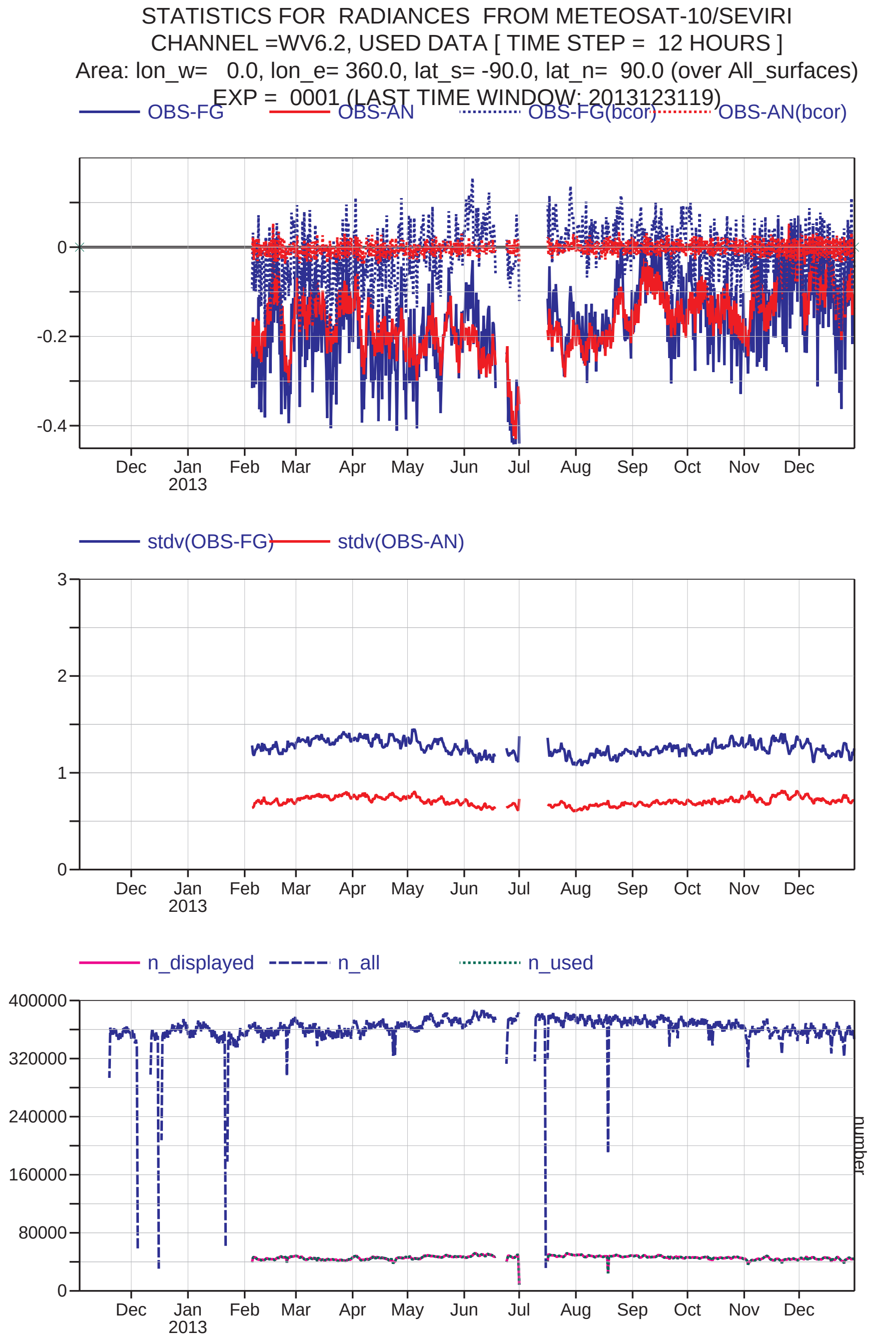

Figure 7: Long time series of first-guess and analysis departure statistics, in K, for the active assimilation of Meteosat-10 WV-ASR from February to December 2013.

5 Evaluation of the model humidity errors growth within the 4D-Var window

Work has started to investigate the feasibility of extracting information about the model error from observations. Due to their excellent temporal resolution, geostationary satellite data are an obvious candidate to start studying the growth rate of the model humidity errors within the 4D-Var window.

5.1 Motivation: Results from deterministic 4D-Var assimilation

Figure 8 shows standard deviations of the first guess and analysis departures as a function of time within both 21 UTC - 9 UTC and 9 UTC - 21 UTC analysis windows of the 4D-Var system for SEVIRI WV radiances as calculated from the operational ECMWF analysis for July 1-31, 2011 (model cycle 37R2). The standard deviation of first guess departures increases from approximately 0.9 K to 1.4 K over each of the two 12-h assimilation windows: observations at the beginning of the assimilation window have smaller first guess departures, whereas observations towards the end of the assimilation window show the largest first guess departures.

The temporal variation of standard deviation of analysis departure show a closest fit to observations at about the mid-point of the 12-h assimilation window and this increase at both ends of the assimilation window, suggesting a sign of a model error (Talagrand, 1998).

The strong constraint 4D-Var used here is based on the perfect model assumption, where any discrepancy between the model and the data is attributed to errors in the background and in the observational state. If the model was perfect, the fit should be constant in time since it would depend only on the accuracy of the observations. When model error is present, the model drifts away from the correct solution and the discrepancy with observations increases with time (Trémolet, 2007).

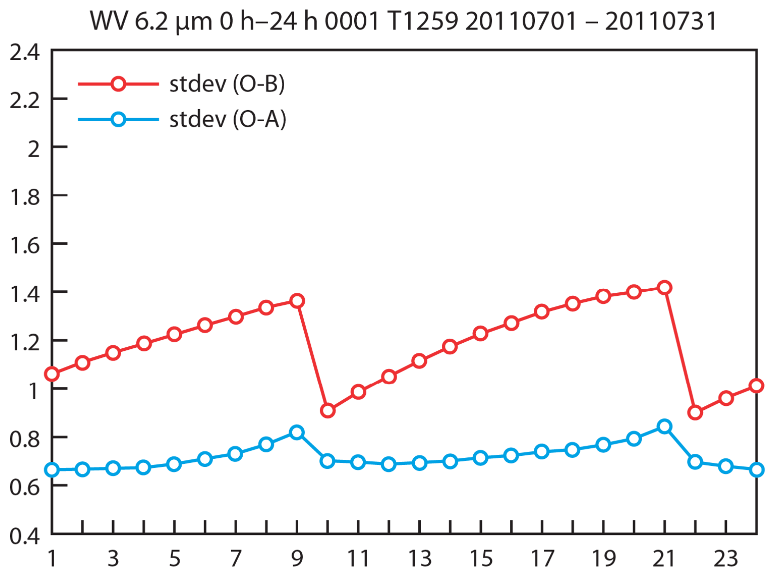

Figure 8: 24-h temporal evolution of the standard deviations of the first guess (red) and analysis (blue) departures for all clear SEVIRI radiances in water-vapour channel at 6.2 m calculated from the operational ECMWF analysis for July 1-31, 2011. The 00 UTC analysis of the 12-hour 4D-Var analysis uses observations in the time window 21-9 UTC, while the 12 UTC analysis uses observations in the time window 9-21 UTC.

The use and rejection of observations is an essential part of any 4D-Var data assimilation system. The subsequent section details the quality control decisions by which geostationary CSR are screened out. We will investigate their variation as a function of the position of the observation in the assimilation window and whether this information can be used to better tune quality control checks of the strong constraint 4D-Var formulation.

5.2 Quality control decisions applied to geostationary radiances

Various quality control checks are applied to the observations prior to and during the 4D-Var analysis. Along with the background and analysis departures, the quality control information is stored with the observations and can be used for post-processing investigations.

The current operational 4D-Var ECMWF system uses a 12-hour assimilation window and 12 images from each of the geostationary satellites are used for each analysis. Depending on the instrument, one or two channels peaking in the water vapour absorption band were used, with maximum sensitivity in the mid-to-upper troposphere. For the studied period (*i.e.*, July 2011), CSR from Meteosat-7/-9, GOES-11/13 and MTSAT-2 that pass quality control checks were used in the analysis. Quality control checks include:

- **Preliminary checks:** serve to identify errors that can occur when measurements are recorded or transmitted (*i.e.*, completeness of reports).
- **Thinning:** serves to prevent effects of spatially correlated observation errors that are not explicitly accounted for by the analysis method. CSR are thinned down to 1.25°(matching roughly the resolution of analysis increments at 125 km).
- **Blacklist rules:** are applied in order to exclude observations that are expected to have a negative impact on the analysis. CSR with satellite zenith angle greater than 60°, or above high terrain (*i.e.*, elevation higher than 1500 m) are rejected. Additionally, two criteria are applied to exclude CSR observations in the WV channel, which mainly occur through cloud contamination:

  – The percentage of clear pixels provided with each observation is used as an indicator of possible cloud contamination. This quality indicator is specific for each dataset, as the data providers use different methods to assign a cloud flag to the observations (*i.e.*, 70% for Meteosat and GOES and 50% for MTSAT satellites).

  – Data over sea for which the model departure in the window channel is outside [-3K, 3K] range is rejected. This test cannot be used over land because the uncertainty in the model skin-temperature is too large.

  Subsequent blacklist decisions, based on prior knowledge about instrument performance are applied to particular datasets, as for example the treatment of the GOES-13 data that is, a seven-hours exclusion around local midnight, every day of the year and the treatment of some of the Meteosat-7 data slots that are blacklisted during the spring and autumn eclipses. For more details on the blacklist decisions applied to geostationary radiances the reader is referred to Lupu and McNally (2011, 2012), Peubey *et al.* (2009), Peubey and McNally, (2009), Munro *et al.*, (2004) and Köpken *et al.*, (2004).

- **Quality control tests:** The *background check* eliminates any observation whose departure from the background exceeds a prescribed threshold, which is proportional to the expected departure based on error statistics for background and observations. CSR are rejected if the absolute value of the departure of the observed value from the first guess, $\mathbf{y}$ - $\boldsymbol{H}(\mathbf{x}_b)$, is bigger than $\lambda\sqrt{\sigma_o^2+\sigma_b^2}$, whith λ (set to 2.25 K) being defined as the rejection criteria, σ_o the observation error standard deviation (set to 2 K) and σ_b the background error standard deviation. This background check for CSR data is only applied in the first trajectory of each 4D-Var cycle, as for all other observation types. Then, in the course of each minimization, the *variational quality control* (VarQC, Andersson and Järvinen 1999) already applied to all other observation types is also applied to CSR observations. Any observation that leads to large departures that are deemed inconsistent with other nearby observations, has its weight artificially reduced in the analysis.

Observations that fail any of these checks are flagged for exclusion from further analysis. To illustrate the impact of quality-control decisions on CSR usage, figure 9 shows the percentage of data rejected due to the above selection rules. Focussing on the Meteosat-9 SEVIRI radiances it can be seen that 86% of the data is flagged for exclusion (*i.e.*, 47.97% due to report rejected, 37.48% due to the blacklist rules and 0.56% due to the quality control tests) and only 14% of the data is used in the analysis .

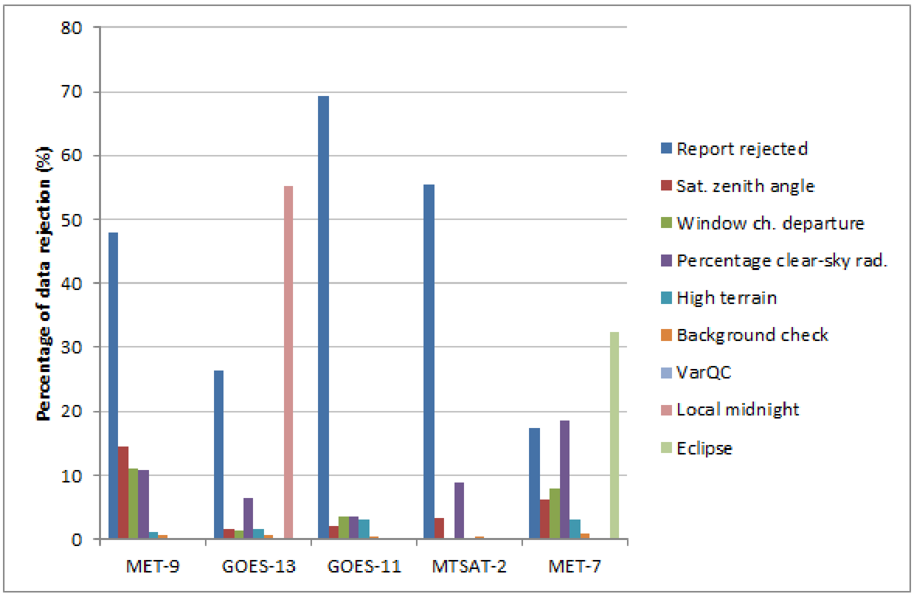

Figure 9: Percentage of CSR flagged for rejection in ECMWF operations on July 1, 2011 at 00 UTC. All percentages are relative to the total data counts.

The analysis of rejected observations as a function of the position of the observation in the 0 UTC assimilation window has indicated that the percentage of Meteosat-9 CSR rejected rises from 6.88% at the begining of the assimilation window to 7.1% at the end of the assimilation window. Both, the background check and the departure in the window channel criterias rejects more data towards the end of the assimilation window (Fig. 10). Initial trials using a relaxed background check criteria (λ set to 6 K) or a time dependent departure in the window channel criteria lead to an increased number of assimilated Meteosat-9 radiances in the second half of the assimilation window but, did not suggest potential on improving the standard deviation of first guess departures of active assimilated Meteosat-9 observations. Due to the evolution of the background error covariance matrix across the assimilation window, observations assimilated towards the end of the window are more influential than observations assimilated at the beginning of the window (*e.g.*, Peubey and McNally, 2009).

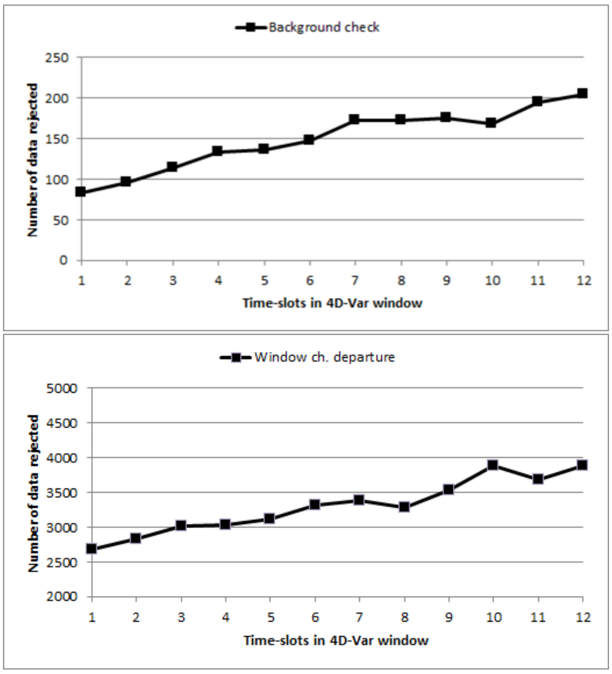

Figure 10: Number of data rejected as function of the position of the observation in the assimilation window : a) background check; b) window channel departure. Results are valid for 1 July 2011 at 0 UTC.

An increase of the size of first guess departures as a function of the position of the observation in the assimilation window has been noted for AMSU-A, MHS and HIRS observations (Bormann and Bonavita, 2013). The increase is more important for the humidity sounding channels of MHS, but relatively small for the temperature sounding channels of AMSU-A.

At ECMWF, an ensemble of data assimilation (EDA) is used to estimate the background errors for the deterministic 4D-Var (Bonavita *et al.*, 2012). The EDA has been recently used to directly estimate background errors in radiance space, for use in quality control decisions for AMSU-A, MHS and HIRS radiance assimilation (Bormann and Bonavita, 2013). At the time of their study (model cycle 38R2), the background error covariance statistics consisted of a static part (the correlations) and a dynamic part (the variances) that represent the flow-dependent component. The general conclusion was that the EDA spread does not grow as quickly as observation departures do. The re-tuning of the background check limits together with the changes to the estimates for the background errors in radiance space allows the use of more AMSU-A, MHS and HIRS observations. Similar conclusions has been also noted for geostationary radiances which uses the background error estimates from HIRS water vapour channels. This study highlighted that observation-based diagnostics can provide additional evaluation in the calibration of EDA for the provision of background error used in data assimilation. Those changes opens the possibility of better describing the evolution of first-guess error over the assimilation window from the evolution of the EDA spread over the assimilation window.

The representation of the background error has been further extended with the more recent upgrade (model cycle 40r1) to compute flow-dependent estimates of background error correlation structure. The EDA has been also enhanced from 10 to 25 members to allow the cycling of background error covariances used in 4D-Var. Therefore further work is needed to establish if the new estimates for the background errors together with a more fundamental change to the quality control (*e.g.*, Huber norm, Tavolato and Isaksen, 2010) will help to reduce the number of geostationary radiance rejections towards the end of the assimilation window.

Being able to correct for the part of the forecast error that is due to the model uncertainties is one of the reasons why the weak-constraint 4D-Var formulation is currently receiving considerable attention at ECMWF. Accounting for model error requires the proper estimation of its statistics as described in the model error covariance matrix, which is still a major difficulty. One benefit of weak constraint 4D-Var is that it should allow for a longer assimilation window, which would allow for more past and future observations to contribute to a better adjustment of the model analysis trajectory. Earlier work performed by Trémolet, (2007) shows that, when model error is accounted for, the weak constraint 4D-Var does fit observations (*e.g.*, wind prolers over North America) more uniformly over the assimilation window. The fit of the background to the observations is also improved but mostly in the first part of the assimilation window. His results indicate the importance of taking into account the information that the model is not perfect through the model-error covariance matrix.

6 Summary

This report is the final report of the EUMETSAT fellowship on the assimilation of clear and all-sky radiance products from geostationary satellites in the ECMWF 4D-Var data assimilation system. The fellowship had two aspects: an operational one dealing with the maintenance of the geostationary network of clear and all-sky radiances assimilated in the ECMWF operational suite, and a more research orientated one, which in particular aimed to understand and improve the impact of geostationary radiance observations on ECMWF analyses and forecasts.

This last year, the maintenance aspect has involved adapting the system for the monitoring and assimilation of CSR from GOES-15 and ASR from Meteosat-10, validating these data and ensuring a smooth transition between satellites in operations. The blacklist rules required continuous maintenance to account for outages occured in the geostationary network. The software producing the simulated images of geostationary satellite data has been maintained to follow the changes in the geostationary operational network and tested with the latest model updates.

Follow-on satellites are scheduled for launch in the future. JMA plans to launch Himawari-8 (summer 2014) to commence its operation in 2015 when MTSAT-2 is scheduled to complete its period of operation. The launch of Himawari-9 for in-orbit standby is also planned for 2016. JMA will continue to operate Himawari-8 and -9 at around 140°E covering the East Asia and Western Pacific regions, as with the current MTSAT series. The next generation of geostationary GOES satellites (GOES-R) is scheduled to be launched in 2015. NOAA/NASA will maintain with the GOES-R series the 2-satellite system implemented by the current GOES series (75°W and 137°W longitudes for GOES-East and GOES-West, respectively). EUMETSAT MSG-4 satellite, the last satellite in the MSG series will be launched in 2015 and stored in orbit until it is required to replace Meteosat-10.

Radiance measurements from geostationary infrared sensors from the water-vapour channel provide valuable information on the mid- and upper tropospheric humidity field and have a proven ability to provide wind information. In a multivariate data assimilation system, like the 12-hour window 4D-Var used at ECMWF, wind information can be derived from radiance observations, even though the radiances are not directly sensitive to tropospheric wind. This influence can occur primarily through two mechanisms: a) the radiances can affect the mass fields of the atmosphere leading to adjustments in the dynamics (either through the forecast model or through balance constraints included in the background error formulation); b) the assimilation system has the freedom to adjust the wind field of the initial conditions directly in order to achieve a better agreement between observations and a moving humidity structure in the model fields over the time window used in the 4D-Var (*tracing effect*).

As with the clear sky case the primary focus for SEVIRI all-sky radiances has been on the 4D-Var wind tracing capability, but above the cloud top in overcast scenes (Lupu and McNally, 2012). The complementarity of 4D-Var tracer information and AMVs has been studied, and detailed comparison with cloudy AMVs and CSR have been performed to understand how the wind information from those data sources is distributed in the vertical. This study provides an initial base for future work towards evaluating the ability to trace the 4D-Var wind advection of cloud signatures in line with the development of explicit cloud control vector variables in the data assimilation system. The general framework in which cloudy geostationary data will be studied will follow the evolution of that used for other infrared data from overcast to the all-sky route.

Efforts have been also devoted to investigate the dynamical impact of SEVIRI ozone-sensitive radiances from Meteosat-9 on wind analyses. The reader is refered to Lupu and McNally (2013) for further details. We have illustrated the effect of ozone feature tracing in the 4D-Var and highlighted that, if the dynamical link between the ozone and the rest of the system is enabled, the 4D-Var has the freedom to change the temperature and wind fields, as well as the ozone field itself in order to improve the fit to observed ozone concentrations. Thus, ozone observations, via passive tracing, provide a potentially useful constraint upon the analysis of wind, particularly in the upper troposphere and lower stratosphere. In the full observing system, the assimilation of one additional ozone sensitive channel from SEVIRI improves the fit to other IR ozone data (*e.g.,* HIRS, IASI) but the improvement is not visible in the fit to MLS. The wind analysis and forecast impact is neutral. We do not currently assimilate in ECMWF operations SEVIRI ozone sensitive radiances.

An investigation has started within the ECMWF system in order to exploit the high time sampling of geostationary radiance data (*e.g.,* Meteosat-9) to study the growth rate of the model humidity errors within the 4D-Var window. The temporal evolution of standard deviation of first guess departures on WV channel at 6.2 μm shows an increase of about 0.5 K over the 12-hour assimilation window. Initial trials with a re-tuned background check and with a time dependent departure in the window channel criteria lead to an increased number of assimilated Meteosat-9 radiances in the second half of the assimilation window but, did not suggest potential on improving the standard deviation of first guess departures of active assimilated Meteosat-9 observations.

Recent developments in the ECMWF system allows the estimation of the background error in radiance space from the EDA spread. More investigations might be done in order to work out the possibility of improving the exploitation of water vapour satellite data. One area involves extending the Huber-norm variational quality control scheme to include humidity sensitive geostationary radiances.

7 Acknowledgements

Cristina Lupu's work at ECMWF was funded by the EUMETSAT Research Fellowship Programme. The help of Ioannis Mallas (ECMWF) in pre-processing GOES-15 and Meteosat-10 data is gratefully acknowledged. Pascal Brunel (Météo France) and Marco Matricardi (ECMWF) provided GOES-15 and Meteosat-10 coefficients files. Tony Schreiner (CIMSS) and Tim Schmit (NOAA/NESDIS) provided valuable feedback on the GOES-15 data quality. Phil Watts, Tim Hewison and Rolf Stuhlmann from EUMETSAT are thanked for fruitful discussion and feedback on the Meteosat-10 data quality. Takahito Imai and Yoshi Sato from JMA are thanked for regulary informing us about the planned MTSAT manoeuvres. We very much appreciate support from and discussions related to this work with ECMWF colleagues: Anne Fouilloux, Niels Bormann, Alan Geer, Mohamed Dahoui, Gabor Radnoti, John Hodkinson, Paul Dando, Stephen English and Jean-Noël Thépaut.

References

Andersson, E., and H. Järvinen, 1999: Variational quality control. *Q. J. R. Meteorol. Soc.* **125**, 697-722.

Bormann, N., and M. Bonavita, 2013: Spread of the ensemble of data assimilations in radiance space. Technical memorandum 708, ECMWF, 29pp.

Bonavita, M., L. Isaksen, and E. Hólm, 2012: On the use of EDA background error variances in the ECMWF 4D-Var. *Q. J. R. Meteorol. Soc.*, **138**, 15401559.

Köpken, C., G. Kelly, and J-N. Thépaut, 2004: Assimilation of Meteosat radiance data within the 4D-Var system at ECMWF: Data quality monitoring, bias correction and single-cycle experiments. *Q. J. R. Meteorol. Soc.* **130**, 2293-2313.

Lupu, C., and A. McNally, 2011: Assimilation of radiance products from geostationary satellites: 1-year report, No. 21, EUMETSAT/ECMWF Fellowship Programme Research Reports, 27pp.

Lupu, C., and A. McNally, 2012: Assimilation of cloud-affected radiances from Meteosat-9 at ECMWF, No. 25, EUMETSAT/ECMWF Fellowship Programme Research Reports, 33pp.

Lupu, C., and A. McNally, 2013: Wind tracing with SEVIRI ozone sensitive radiances, No. 31, EUMETSAT/ECMWF Fellowship Programme Research Reports, 23pp.

McNally, A., 2009: The direct assimilation of cloud-affected satellite infrared radiances in the ECMWF 4D-Var. *Q. J. R. Meteorol. Soc.*, **135**, 1214-1229.

Munro, R., C. Köpken, G. Kelly, J-N. Thépaut, and R. Saunders, 2004: Assimilation of Meteosat radiance data within the 4D-Var system at ECMWF: Assimilation experiments and forecast impact. *Q. J. R. Meteorol. Soc.* **130**, 2277-2292.

Peubey, C., and A. P. McNally, 2009: Characterization of the impact of geostationary clear sky radiances on wind analyses in a 4D-Var context. *Q. J. R. Meteorol. Soc.* **135**, 1863-1876.

Peubey, C., A. P. McNally, J.-N. Thépaut, S. Uppala, and D. Dee 2009: Updates in the assimilation of geostationary radiances at ECMWF. Proceedings of the 2009 EUMETSAT Meteorological Satellite Conference, Bath, UK, 5pp.

Schmetz, J., P. Pili, S. Tjemkes, D. Just, J. Kerkmann, S. Rota, and A. Ratier, 2002: An Introduction to

Meteosat Second Generation (MSG). *Bull. Amer. Meteor. Soc.*, **83**, 977-992.

Dee, D. P., 2004: Variational bias correction of radiance data in the ECMWF system. Proceedings of the ECMWF workshop on assimilation of high spectral resolution sounders in NWP, 28 June-1 July 2004. Reading, UK.

Tavolato, C., and L. Isaksen, 2010: Huber norm quality control in the IFS. ECMWF Newsletter, 122, 2731.

Trémolet, Y., 2007: Model-error estimation in 4D-Var. *Q. J. R. Meteorol. Soc.*, **133**, 1267-1280.

APPENDIX I: Accronyms and abbreviations

4D-Var	Four-dimensional variational data assimilation
AMVs	Atmospheric Motion Vectors
AMSU-A	Advanced Microwave Sounding Unit
CIMSS	Cooperative Institute for Meteorological Satellite studies
CSR	Clear Sky Radiances
ASR	All Sky Radiances
ECMWF	European Centre for Medium Range Weather Forecast
EDA	Ensemble of Data Assimilation
EUMETSAT	European Organisation for the Exploitation of Meteorological Satellites
GOES	Geostationary Operational Environmental Satellite
HIRS	High Resolution Infrared Radiation Sounder
IASI	Infrared Atmospheric Sounding Interferometer
IFS	Integrated Forecasting System
IR	Infrared
JMA	Japan Meteorological Agency
LRIT	Low Rate Information Transmission
MLS	Microwave Limb Sounder
MHS	Microwave Humidity Sounder
MTSAT	Multifunctional Transport Satellites
NOAA	National Oceanic and Atmospheric Administration
NWP	Numerical Weather Prediction
RMS	Root Mean Square forecast error
RTTOV	Radiative Transfer for TOV
SEVIRI	Spinning Enhanced Visible and Infrared Imager
VarBC	Variational Bias Correction
VarQC	Variational Quality Control
WV	Water vapour